Journal of Physics: Conference Series **447** (2013) 012013 doi:10.1088/1742-6596/447/1/012013

CP violation at the B factories

John Walsh, on behalf of the Babar and Belle Collaborations
INFN, Sezione di Pisa, Largo Pontecorvo 3, 56127 Pisa, Italy
E-mail: john.walsh@pi.infn.it

Abstract. One of the primary goals of the B factory experiments was to measure and study CP violation in B meson decays, a goal which has been met very successfully. This paper reports on recent measurements of CP violation at the Babar and Belle experiments. Particular focus is placed on the measurements of the three angles of the Unitarity Triangle, β, α and γ.

1. Introduction

The B factories, asymmetric e^+e^- colliders operating mainly at center-of-mass energy of 10.58 GeV, corresponding to the mass of the $\Upsilon(4S)$ resonance, were constructed in the late 1990's at SLAC in California and at KEK in Japan. The principal objective of the B factory experiments, Babar and Belle, was the study CP violation in B meson decays. Up to that time, CP violation had only been seen in kaon decays [1] and for many years the study of CP violation was confined to the kaon system, with its inherent difficulties owing to hadronic uncertainties. These difficulties were greatly reduced in the B meson system, due to the much larger mass of the B meson. Furthermore, CP violation was expected to be much larger in the B system, allowing a large number of precise measurements.

The numerous measurements of CP violation made by the Babar and Belle experiments have largely confirmed the mechanism by which CP violation occurs in the Standard Model (SM). The SM has been tightly overconstrained by the CP violation measurements and it has withstood this exacting test: no indications of new physics (NP) beyond the SM have been found.

In these proceedings, I will review CP violation measurements at the B factories. After a brief introduction to CP violation within the Standard Model, followed by some general comments on experimental techniques, I will discuss selected key measurements at Babar and Belle. The focus will be on the determination of the three angles of the Unitarity Triangle, β, γ and α. In Belle papers, these angles are referred to as ϕ_1, ϕ_3 and ϕ_2, respectively. I will use the Babar convention in these proceedings.

2. The CKM matrix and the Unitarity Triangle

The Cabibbo-Kobayashi-Maskawa (CKM) matrix [2, 3] describes the relations among the quark mass eigenstates and the weak interaction eigenstates. Thus, it describes the coupling strength of quarks to the charged weak interaction. In the SM, the CKM matrix is a 3×3 unitary matrix. Its complex values V_{ij} are not specified by the SM, but must be determined by experiment. The property of unitarity leads to constraints which reduce the number of independent parameters to four. A convenient parametrization of the CKM matrix from Wolfenstein [4] shows explicitly

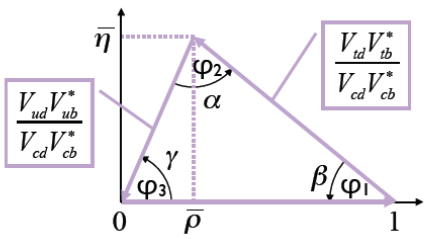

Figure 1. Unitarity triangle.

the dependence on only four independent quantities:

$$V_{CKM} = \begin{pmatrix} 1-\lambda^2/2 & \lambda & A\lambda^3(\rho-i\eta) \\ -\lambda & 1-\lambda^2/2 & A\lambda^2 \\ A\lambda^3(1-\rho-i\eta) & -A\lambda^2 & 1 \end{pmatrix} + O(\lambda^4) \quad (1)$$

At the time of B factory construction, the parameters λ and A were well measured, while ρ and η were essentially unknown.

One of the six unitarity constraints on the CKM matrix may be written as:

$$V_{ud}V_{ub}^* + V_{cd}V_{cb}^* + V_{td}V_{tb}^* = 0. \quad (2)$$

We may divide the above relation by $V_{cd}V_{cb}^*$ and express the result in the complex plane as a triangle, known as the Unitarity Triangle (UT), as shown in Figure 1. The apex of the triangle is positioned at $\bar{\rho}+i\bar{\eta}$ (the barred versions of ρ and η take into account higher orders of λ). The UT angles β, γ and α give rise to CP-violating asymmetries, which can be measured at the B factories. Measurements of these three angles are discussed in the following sections. The two (non-trivial) sides can also be measured at the B factories, using semileptonic and rare decays, as well as $B^0\bar{B}^0$ mixing.

3. Experimental considerations

The Babar and Belle detectors have been described in detail elsewhere [5, 6] and will not be discussed here. Each of the two experiments does an excellent job of reconstructing charged tracks and decay vertices, detecting photons even down to low energy ($\sim$ 30 MeV) and performing particle identification to reconstruct electrons, muons, pions, kaons and protons.

The measurement of time-dependent CP asymmetries is the main tool by which the angles β and α are measured at the B factories. When the $\Upsilon(4S)$ decays to a $B^0\bar{B}^0$ pair, one of the B's is typically fully reconstructed in a CP-eigenstate, for example $B^0 \to J/\psi K_S^0$. The flavor of the other B in the event is "tagged" by identifying some of its decay products, typically a lepton or kaon. The flavor at the time of decay can be deduced from the charge of the lepton or kaon. The third ingredient in the measurement of time-dependent CP-aymmetries is a measurment of the time elapsed between the two B decays. This is determined by precisely reconstructing the decay vertices of both B's in the event and using the known boost of the $\Upsilon(4S)$ to determine the proper time. The CP-asymmetry is then computed at a function of the time:

$$A_{CP}(t) = \frac{N(\bar{B}^0 \to f_{CP}) - N(B^0 \to f_{CP})}{N(\bar{B}^0 \to f_{CP}) + N(B^0 \to f_{CP})} \quad (3)$$

$$= S_f \sin\Delta mt - C_f \cos\Delta mt \quad (4)$$

Where the coefficients S_f and C_f are related to UT angles in a mode-dependent way. This asymmetry, as we shall see, can be related to the UT angles β and α. For the third angle γ, the most powerful methods use time-integrated asymmetries of the tree-level decays $B \to D^{(*)}K^{(*)}$.

Table 1. Signal yields in the different modes used in Belle's $\sin 2\beta$ measurement.

Final state	Signal yield
$J/\psi K^0_S$	12649 ± 114
$\psi(2S)(\ell^+\ell^-)K^0_S$	904 ± 31
$\psi(2S)(J/\psi\pi^+\pi^-)K^0_S$	1067 ± 33
$\chi_{c1}K^0_S$	940 ± 33
$J/\psi K^0_L$	10040 ± 154

4. Measurement of β

The angle β is the most precisely measured of the three UT angles, due to the very favourable decay mode which is sensitive to it: $B^0 \to J/\psi K^0_S$. Additionally, $\sin 2\beta$ can be measured using $b \to s(q\bar{q})$ decays ($q = u, d, s$), also known as "gluonic penguins". I will discuss measurements of both types in this section.

4.1. $B^0 \to (c\bar{c})K^0$ modes

The decay mode $B^0 \to J/\psi K^0_S$, which has a relatively large branching fraction, is fully reconstructed with very low background due to the distinctive decay mode $J/\psi \to \ell^+\ell^-$ where ℓ is either a muon or an electron. Furthermore, this channel has a clean theoretical interpretation as well. Since only one decay amplitude contributes to this mode, the coefficients of Eq. 4 can be simply expressed as

$$S_f = \sin 2\beta \tag{5}$$

$$C_f = \frac{1 - |\lambda_f|^2}{1 + |\lambda_f|^2} \tag{6}$$

where $\lambda_f = (q/p)(\bar{A}_f/A_f)$, p and q are complex constants that relate the B flavour eigenstates to the mass eigenstates, and $\bar{A}_f/A_f$ is the ratio of the decay amplitudes of $\bar{B}^0$ and B^0 to the final state f. For this channel, C_f is expected to be zero, but it is typically allowed free in the fit as a consistency check.

Belle's final measurement of $\sin 2\beta$ using the $B^0 \to (c\bar{c})K^0$ modes is based on a dataset of 772 million $B^0\bar{B}^0$ pairs [7]. Table 1 shows the final states analyzed along with the event yield for each channel, while Fig. 2 shows the beam-constrained mass (or reconstructed B momentum for the $J/\psi K^0_L$ mode) for selected candidates. The selected samples are divided into two sub-samples, depending on whether the tagged B meson was a B^0 or $\bar{B}^0$. Figure 3 shows the distribution of Δt for the B^0- and $\bar{B}^0$-tagged sub-samples superimposed. The sinusoidal shape of the time-dependent CP-asymmetry (Eq. 4) is clearly evident as shown in the lower half of the figure. The CP-violating parameters, $S_f = \sin 2\beta$ and C_f, obtained from a fit to the Δt distributions, are shown in Table 2. For comparison, we also show the results of a similar analysis from Babar [8], which was based on a somewhat smaller data sample (465×10^6 $B\bar{B}$ events).

4.2. $b \to s(q\bar{q})$ modes

In the Standard Model the $b \to s(q\bar{q})$ modes are dominated by the so-called penguin amplitude, which has the same weak phase as the $b \to s(c\bar{c})$ amplitude. Figure 4 shows the Feynman diagram for the SM decay. These modes are particularly interesting since they are in principle sensitive to New Physics, with new heavy particles participating in the penguin loop. However, the situation with these decays is more complicated because suppressed SM diagrams cannot be neglected, contributing from 1–10% to the CP-violating parameter S_f, which gets shifted relative the same quantity measured in $b \to s(c\bar{c})$ decays:

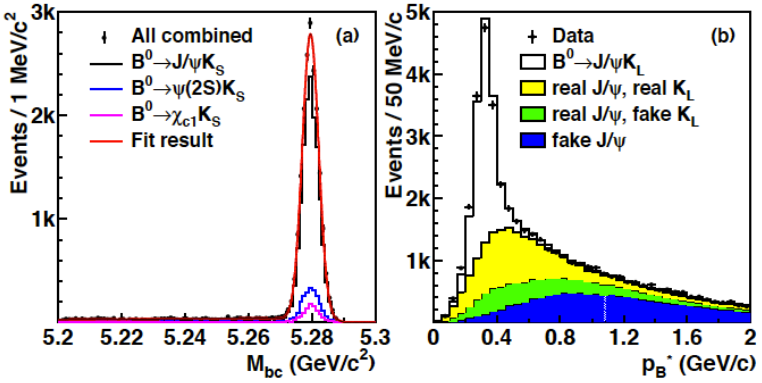

Figure 2. The beam-constrained mass for the $(c\bar{c})K^0_S$ modes (left) and the reconstructed B momentum (center-of-mass frame) for the $J/\psi K^0_L$ mode (right).

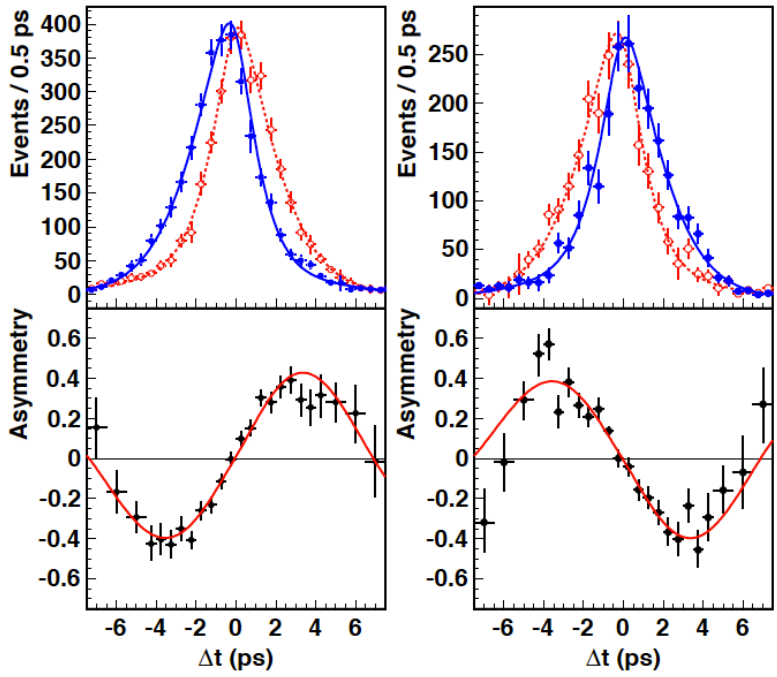

Figure 3. The distribution of Δt (top) for $\bar{B}^0$ decays (blue) and B^0 decays (red). The bottom shows the time-dependent CP asymmetry. CP-odd modes are shown on the left, while the CP-even mode is on the right.

Table 2. Fit results of CP-violating parameters from $B^0 \to (c\bar{c})K^0$ modes from Belle and Babar. The first uncertainty quoted is statistical, the second systematic. In Belle notation the angle β is called ϕ_1 and $\mathcal{A}_{CP} = C_f$ (defined in Eq. 6).

Experiment	$\sin 2\beta$	C_f
Belle	$0.667 \pm 0.023 \pm 0.012$	$-0.006 \pm 0.016 \pm 0.012$
Babar	$0.678 \pm 0.028 \pm 0.012$	$0.024 \pm 0.020 \pm 0.016$

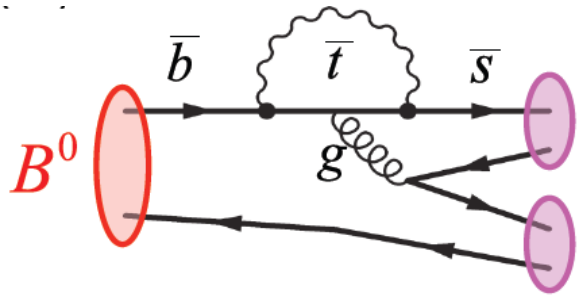

Figure 4. Feynman diagram of $b \to s(q\bar{q})$ transition.

Table 3. Results on $\sin 2\beta_{\rm eff}$ from the time-dependent Dalitz plot analysis of $B^0 \to K^+K^-K_S$.

Renonance	$\sin 2\beta_{\rm eff}$
ϕK_S	$(21 \pm 6 \pm 2)^\circ$
$f_0 K_S$	$(18 \pm 6 \pm 4)^\circ$
non–ϕ, non–f_0	$(20.3 \pm 4.3 \pm 1.2)^\circ$

$$S_{sc\bar{c}} = S_{sq\bar{q}} + \Delta S_{SM} = -\eta_{CP} \sin 2\beta \tag{7}$$

Any New Physics effects would give an additional contribution to $S_{sq\bar{q}}$. The quantity $-\eta_{CP} S_{sq\bar{q}}$ is often referred to as $\sin 2\beta_{\rm eff}$.

Early measurements of $\sin 2\beta_{\rm eff}$ using several channels seemed to indicate a discrepancy between $\sin 2\beta$ and $\sin 2\beta_{\rm eff}$, at the level of approximately 2σ [9]. Since then analysis techniques for these modes have progressed significantly. One such advanced analysis is Babar's measurement of $\sin 2\beta_{\rm eff}$ using a Dalitz plot analysis of the decay $B^0 \to K^+K^-K_S$ [10]. This final state is in fact a superposition of several resonant modes, for example $B^0 \to \phi K_S$ and $B^0 \to f_0 K_S$ and the Dalitz structure is used to separate the different contributions to CP violation. The Dalitz plot analysis is also able to measure $\cos 2\beta_{\rm eff}$, which eliminates an ambiguity between $\beta_{\rm eff}$ and $90^\circ - \beta_{\rm eff}$. Details on the Dalitz plot model can be found in [10].

Figure 5 shows the Dalitz plot distribution of selected $B^0 \to K^+K^-K_S$ events. The complex amplitude coefficients for the different resonances included in the model are derived from this fit. Flavour tagging of the other B meson in the event is applied in the usual way, allowing the separation of B^0 and $\bar{B}^0$ decays. Figure 6 shows the resulting time-dependent asymmetry, both for the $\phi(1020)$ region (left) and the region where the $\phi(1020)$ is excluded (right). Results for $\sin 2\beta_{\rm eff}$ were extracted for the events consistent with $B^0 \to \phi K_S$, $B^0 \to f_0 K_S$ and the region excluding these two decay mode. The results are presented in Table 3.

5. Measurement of γ

The angle γ of the Unitarity Triangle is generally measured using the tree-level decays $B \to D^{(*)}K^{(*)}$. There are three primary methods used to measure γ: GGSZ, GLW and ADS. The methods generally expoit the interference between two different amplitudes that can give rise to a particular final state. I will describe analyses using the GGSZ and GLW methods in the following.

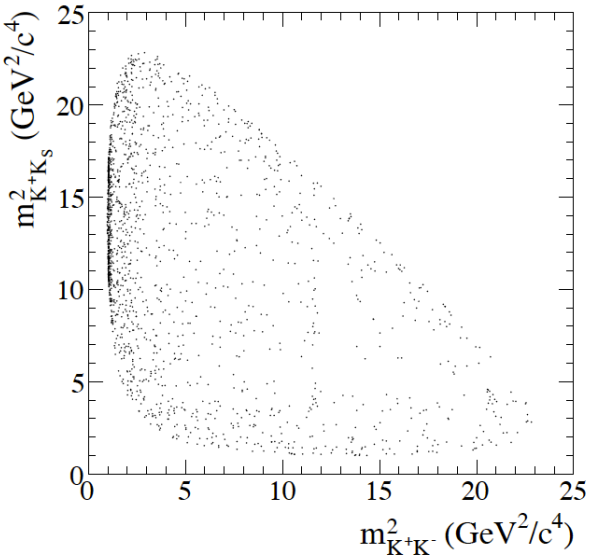

Figure 5. Dalitz plot for $B^0 \to K^+K^-K^0_S$ decays.

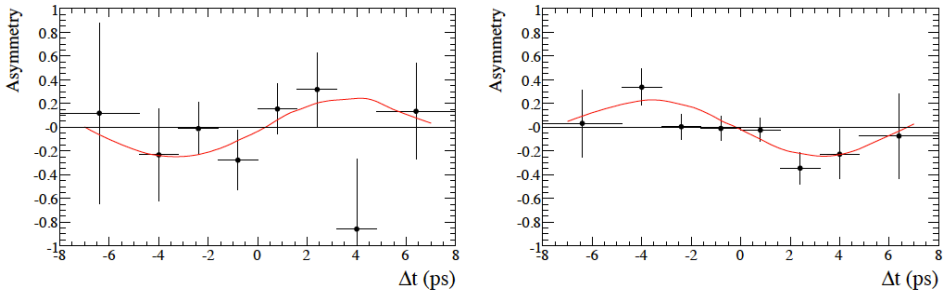

Figure 6. Time-dependent CP-asymmetry for $B^0 \to K^+K^-K^0_S$ events in the $\phi(1020)$ region (left) and for events outside the $\phi(1020)$ region (right).

5.1. GGSZ (Dalitz) method

The GGSZ method [11] exploits the interference between color-favoured and color-suppressed amplitudes in $B \to D^{(*)}K^{(*)}$ decays. In the case of $B^- \to DK^-$ channel, the color-favoured $B^- \to D^0K^-$ ($b \to c\bar{u}s$) and the color-suppressed $B^- \to \bar{D}^0K^-$ ($b \to u\bar{c}s$) amplitudes interfere when the D^0 and $\bar{D}^0$ decay to the same final state. The amplitudes for the B^- and B^+ decays may be written:

$$A_-(m^2_-, m^2_+) = |A(B^- \to D^0K^-)|[A_D(m^2_-, m^2_+) + r_B e^{i\delta_B} e^{-i\gamma} A_D(m^2_+, m^2_-)] \quad (8)$$

$$A_+(m^2_-, m^2_+) = |A(B^+ \to \bar{D}^0K^-)|[A_D(m^2_+, m^2_-) + r_B e^{i\delta_B} e^{+i\gamma} A_D(m^2_-, m^2_+)] \quad (9)$$

The position in the Dalitz plot is specified by $m_\pm = m(K_S, h^\pm)$ where $h = \pi, K$. The two contributions to each amplitude differ by a factor $r_B e^{i(\delta_B \pm \gamma)}$, where r_B is the magnitude of the ratio of the amplitudes $A(B^- \to \bar{D}^0K^-)$ and $A(B^- \to \bar{D}^0K^-)$, and δ_B is the relative strong phase. The analysis presented in [12] considers the self-conjugate D^0 decays to $K_S\pi^+\pi^-$ and $K_SK^+K^-$.

A Dalitz plot analysis of D^0 and $\bar{D}^0$ decays to these final states allows access to the complex amplitude ratios, and thus to the weak and strong phases and r_B. It is useful to express

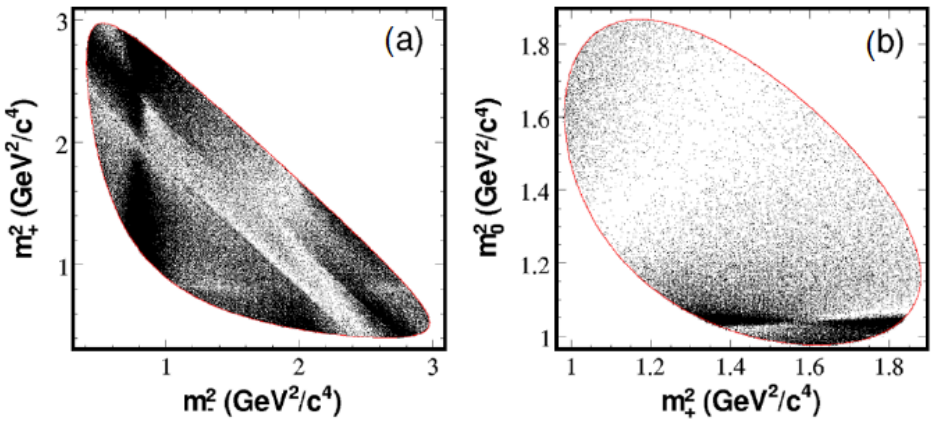

Figure 7. Dalitz plot distributions for a) $D^0 \to K_S\pi^+\pi^-$ and b) $D^0 \to K_S K^+ K^-$.

.

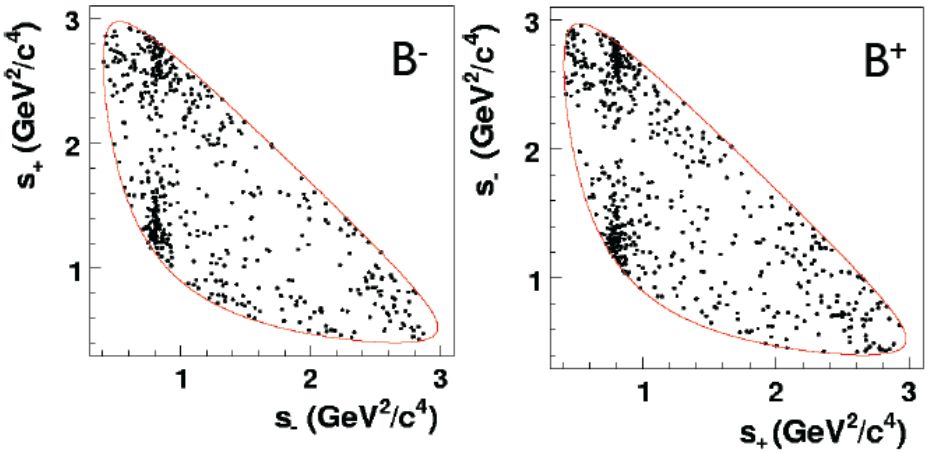

Figure 8. Dalitz plot distributions for (left) $B^- \to D^0 K^-$ and (right) $B^+ \to D^0 K^+$, with $D^0 \to K_S\pi^+\pi^-$.

the unknowns γ, r_B and δ_B in terms of the so-called cartesian variables, which are Gaussian-distributed and hence better behaved statistically:

$$x_\pm = r_B \cos(\delta_B \pm \gamma) \quad (10)$$
$$y_\pm = r_B \sin(\delta_B \pm \gamma) \quad (11)$$
$$z_\pm = x_\pm + i y_\pm \quad (12)$$

The D^0 amplitudes, specified as A_D in Equations 8 and 9 above, are determined from a Dalitz plot analysis performed on a high statistics sample of D^0 mesons produced in the decay $D^{*+} \to D^0\pi^-$ produced in $e^+e^- \to c\bar{c}$ events. The charge of the soft pion in the D^* decay identifies the flavour of the D meson. Figure 7 shows the Dalitz plot distributions for the two final states. The Dalitz analysis performed on these plots provides the values of $A_D(m^2_-, m^2_+)$. These are then used when analyzing the Dalitz plots corresponding to the $B \to DK$ decays, shown in Figure 8. A similar analysis was performed on the related decays $B \to D^*K$ and $B \to DK^*$. The results are summarized in Figure 9, which depicts the measurements

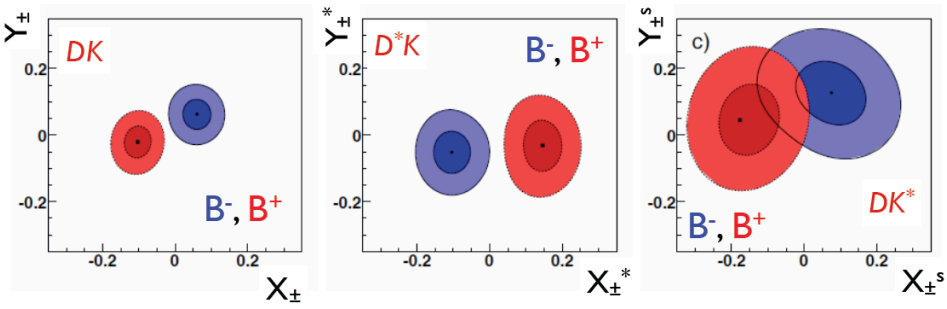

Figure 9. Results, in the $z_\pm$ plane of Babar's GGSZ analysis. The three plots show, from left to right, the results for the DK, D^*K and DK^* final states, respectively. The B^- results are shown in blue, the B^+ results in red.

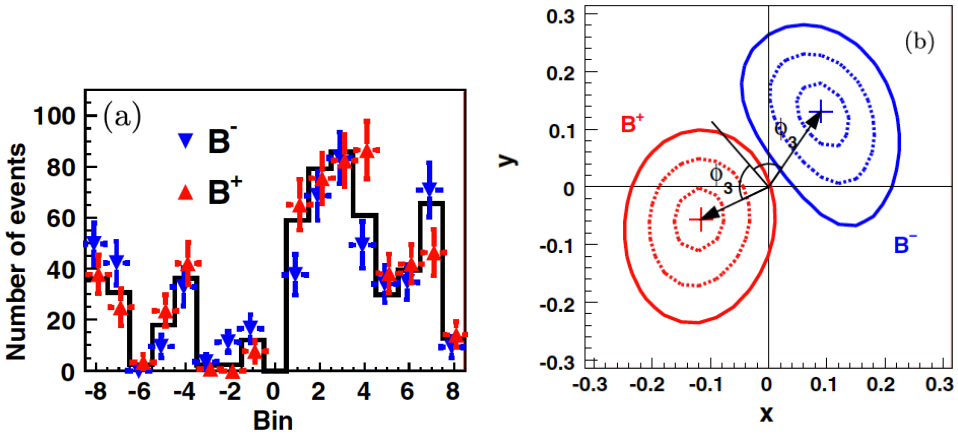

Figure 10. The yields of B^- and B^+ decays into different bins in the Dalitz plot (left), and the resulting values of the cartesian coordinates x and y (right).

of the cartesian variables for the different decay modes. Separation between the B^- and B^+ measurements in the $z_\pm$ plane is an indication of CP violation. For the numerical results for the cartesian variables the reader is referred to reference [12].

The Belle experiment has performed an interesting variation [13] on the GGSZ analysis using the same final states as the Babar analysis. Belle, however, employs a model-independent Dalitz analysis by symmetrically binning the Dalitz plane and forgoing the use of a complicated Dalitz plot model. This method allows the reduction of the primary systematic uncertainty, which comes from the Dalitz model employed. With this method the expected number of events in each Dalitz bin, i is given by:

$$N_i^\pm = hK_i + r_B^2 K_{-i} + 2\sqrt{K_i K_{-i}}(x_\pm c_i + y_\pm s_i) \tag{13}$$

where $-i$ indicates the symmetrically opposite bin to i. K_i is the number of events in bin i from a flavour-tagged sample of $D^{*\pm} \to D\pi^\pm$. The coefficients c_i and s_i, which are related to the strong phase in bin i, are obtained from data taken at the $D^0\bar{D}^0$ threshold by the CLEO experiment.

The results are shown in Figure 10. On the left is plotted the number of B^- and B^+ events found in each of the Dalitz plot bins, with the black histogram representing the expection for both B^- and B^+ in the absence of CP violation. The right plot shows the resulting cartesian

Table 4. Signal yields in different decay modes for Babar's GLW $B \to DK$ analysis. The flavour eigenstate $D^0 \to K^-\pi^+$ is used as the normalization for $R_{CP\pm}$.

D^0 mode	$N(B^\pm \to DK^\pm)$
K^+K^-	367 ± 27
$\pi^+\pi^-$	110 ± 9
$K^0_S\pi^0$	338 ± 24
$K^0_S\omega$	116 ± 9
$K^0_S\phi$	52 ± 4
$K^-\pi^-$	3361 ± 82

variables. These results can also be expressed as:

$$\gamma = (77.3^{+15.1}_{-14.9} \pm 4.1 \pm 4.3)^\circ \quad (14)$$
$$r_B = 0.145 \pm 0.030 \pm 0.010 \pm 0.011 \quad (15)$$
$$\delta_B = (129.9 \pm 15.0 \pm 3.8 \pm 4.7)^\circ \quad (16)$$

where the quoted uncertainties are statistical, systematic, and the error associated with c_i and s_i, respectively.

5.2. GLW method

The GLW method for extracting γ [14] uses decay modes of the D^0 into CP-eigenstates: K^+K^- and $\pi^+\pi^-$, which are CP-even, and $K_S\pi^0$, $K_S\omega$ and $K_S\phi$, which are CP-odd. There are four observables involving the rates of B^- and B^+ decays to CP-odd and CP-even final states:

$$R_{CP\pm} = \frac{\Gamma(B^- \to D^0_{CP\pm}K^-) + \Gamma(B^+ \to D^0_{CP\pm}K^+)}{2\Gamma(B^- \to D^0K^-)} = 1 \pm 2r_b \cos\gamma \cos\delta_b + r_b^2 \quad (17)$$

$$A_{CP\pm} = \frac{\Gamma(B^- \to D^0_{CP\pm}K^-) - \Gamma(B^+ \to D^0_{CP\pm}K^+)}{\Gamma(B^- \to D^0_{CP\pm}K^-) + \Gamma(B^+ \to D^0_{CP\pm}K^+)} = \pm 2r_b \sin\gamma \sin\delta_b / R_{CP\pm} \quad (18)$$

The GLW observables may also be expressed in cartesian variables:

$$A_{CP\pm} = \pm\frac{x_- - x_+}{1 + |z|^2 \pm (x_- + x_+)} \quad (19)$$
$$R_{CP\pm} = 1 + |z|^2 \pm (x_- + x_+) \quad (20)$$

Figure 11 shows the distribution of the discriminating variable ΔE for the Babar GLW analysis of $B \to DK$ [15]. The event yields for the individual channels are shown in Table 4.

Babar finds the following results for the observables:

$$A_{CP+} = 0.25 \pm 0.06 \pm 0.02 \quad (21)$$
$$A_{CP-} = -0.09 \pm 0.07 \pm 0.02 \quad (22)$$
$$R_{CP+} = 1.18 \pm 0.09 \pm 0.05 \quad (23)$$
$$R_{CP0} = 1.07 \pm 0.08 \pm 0.04 \quad (24)$$

where the first uncertainty is statistical and the second systematic.

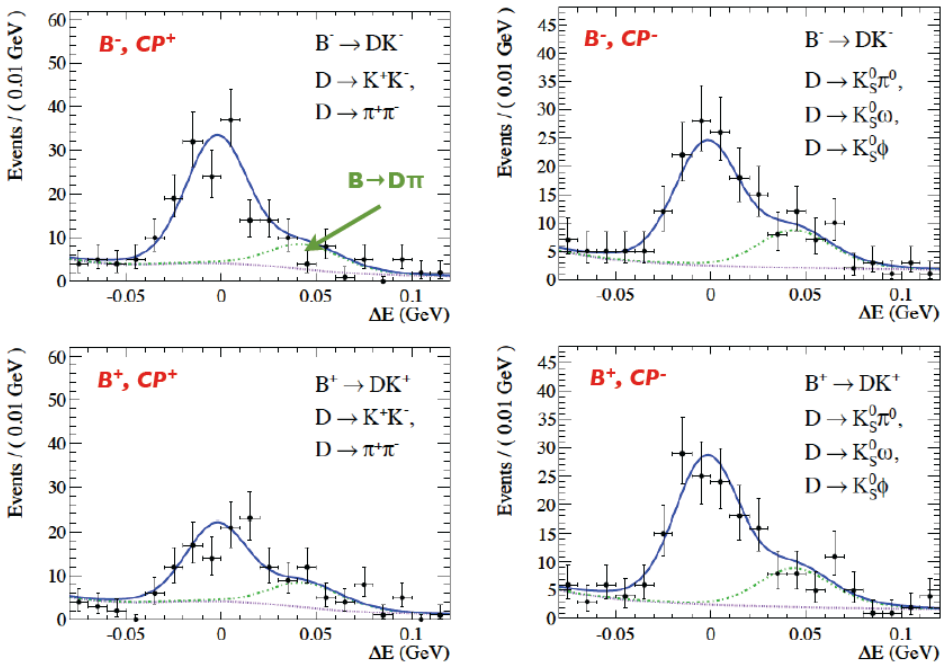

Figure 11. The ΔE distributions of B^- (top row) and B^+ (bottom row) with D decays to CP-even eigenstates (left column) and CP-odd eigenstates (right column).

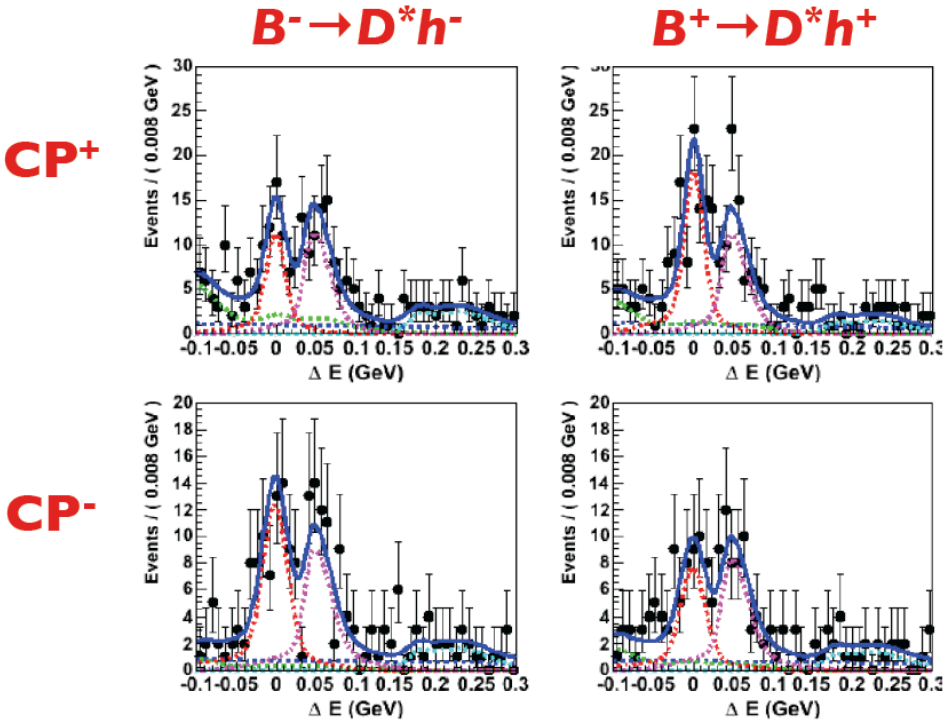

Figure 12. The ΔE distributions of B^- (left column) and B^+ (right column) with D^* decays to CP-even eigenstates (top row) and CP-odd eigenstates (bottom row).

Table 5. Determination of γ achieved by combining measurements.

Experiment	Combined γ (degrees)
Babar	69^{+17}_{-16}
Belle	68^{+15}_{-14}
LHCb	$71.1^{+16.6}_{-15.7}$

Belle has recently performed a GLW analysis using the decay mode $B \to D^*K$ [16]. Figure 12 shows the selected events for B^- and B^+ decays via CP-even and CP-odd D^* decays. Belle finds the following results for the GLW observables:

$$R_{CP+} = 1.19 \pm 0.13 \pm 0.03 \quad (25)$$
$$R_{CP-} = 1.03 \pm 0.13 \pm 0.03 \quad (26)$$
$$A_{CP+} = -0.14 \pm 0.10 \pm 0.01 \quad (27)$$
$$A_{CP-} = 0.22 \pm 0.11 \pm 0.01 \quad (28)$$

5.3. Combination of γ results
The Babar and Belle collaborations have performed dedicated studies to combine all the relevant decay modes and methods to extract the most precise values of γ. The results are first translated into the cartesian variables $x_\pm$ and $y_\pm$. Each channel DK, D^*K and DK^* has its own set of cartesian variables, each of which depends on the common parameter γ. These variables are averaged across the three analysis methods (GGSZ, GLW and ADS), by combining the likelihood functions. As a last step, γ is extracted from the best fit values of the cartesian variables. The results, as tabulated by HFAG [17] are shown in Table 5. Though not covered in this talk, we quote the current LHCb result [18] for comparison.

6. Measurement of α

The UT angle α is measured, in analogy with the β measurements, using time-dependent CP asymmetries in decays to CP eigenstates, for example $B^0 \to \pi^+\pi^-$. However, the situation with α is not so straightforward as with β due to the sizable contribution from more than a single amplitude. In the case of $B^0 \to \pi^+\pi^-$, in addition to the tree diagram, there is a significant contribution from the penguin diagram, with a different CKM structure. The result is that the time-dependent asymmetry measurement yields $\sin 2\alpha_{\rm eff}$, with $\alpha_{\rm eff} = \alpha + \delta$. It turns out that δ can be extracted from an isospin analysis by measuring the branching fractions and time-integrated CP asymmetries of all the channels in the $B \to \pi\pi$ system.

Belle has recently peformed an analysis of the $B^0 \to \pi^+\pi^-$ channel, including the associated isospin analysis [19], based on 772 million $B\bar{B}$ pairs. Figure 13 shows the Δt distributions for B^0- and $\bar{B}^0$-tagged events, along with the time-dependent CP asymmetry. The CP-violating parameters obtained from the fit are:

$$\mathcal{A}_{CP}(B^0 \to \pi^+\pi^-) = +0.33 \pm 0.06 \pm 0.03 \quad (29)$$
$$\mathcal{S}_{CP}(B^0 \to \pi^+\pi^-) = -0.64 \pm 0.08 \pm 0.03 \quad (30)$$

where the quoted uncertainties are statistical and systematic. With the current level of statistics, the isospin analysis of $B \to \pi\pi$ is not very effective in constraining the value of α. Belle excludes the region $23.8^\circ < \alpha < 66.8^\circ$ at the 1σ level.

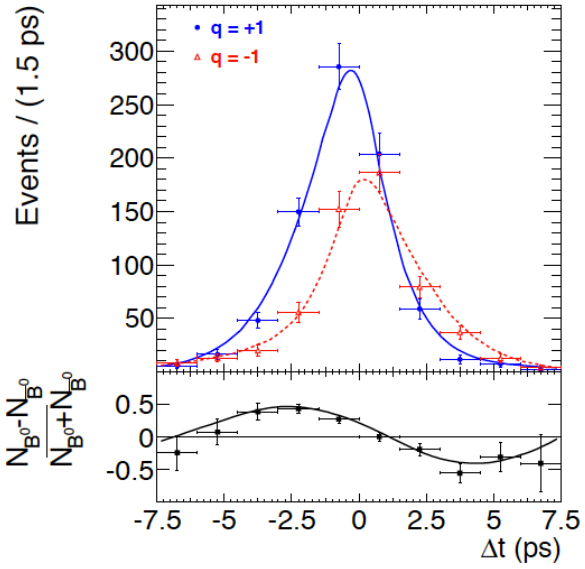

Figure 13. Time-dependent fit results for Belle's $B^0 \to \pi^+\pi^-$ analysis. The top portion shows the background-subtracted δt distribution separately for B^0 (blue) and $\bar{B}^0$ (red) tags. The lower portion of the plot shows the CP asymmetry.

To obtain more stringent constraints on α one must combine results from different modes and different experiments. In particular, the modes $B \to \rho\rho$ and $B \to \rho\pi$ contribute significantly to our knowledge of α. The CKMFitter collaboration has extracted a world average value for α using these measurements from these three channels from the two B factory experiments. They find [20]:

$$\alpha = (88.5^{+4.7}_{-4.4})^\circ \tag{31}$$

7. Global CKM fits

Perhaps the primary goal of the B factories was to make enough measurements in the B physics sector to overconstrain the CKM matrix, with the hope of finding inconsistencies, which would be an indication of physics beyond the Standard Model. Two collaborations, CKMfitter [21] and UTfit [22], have undertaken to combine the many relevant measurents from the B factories, and from other flavour experiments as well, to put stringent tests on the Standard Model. The two collaborations adopt somewhat different statistical methods, while generally using the same inputs. The results obtained are generally in good agreement.

Both collaborations provide averages for the experimental quantities, by averaging over different measurement techniques, decay modes and experiments. Table 6 shows the world averages using direct measurements of the three Unitarity Triangle angles. Additional solutions are present for α (CKMfitter) and γ (UTfit), see the individual collaboration websites for details.

More precise deteriminations of the angles can be made by including the full set of flavour measurements in a global CKM fit. Non-CP violating measurements of the sides of the UT come from semileptonic B decays and mixing in the B^0_d and B^0_s systems. The parameter $|\epsilon_K|$, a measurement of CP violation in kaon decays, is also used in the fit. Figure 14 show the results of such global fits performed by the two collaborations. Table 7 shows the results for the three UT angles and for $(\bar{\rho}, \bar{\eta})$, the coordinates of the apex of the triangle. This fit assumes the validity of the Standard Model, so, for example, the sum $\alpha + \beta + \gamma$ is constrained to 180°.

The fits can be performed without assuming the validity of the Standard Model, indeed,

Table 6. World averages of the UT angles using direct measurments. Measurements are given in degrees.

Collaboraton	β	α	γ
CKMfitter	$21.38^{+0.79}_{-0.77}$	$88.7^{+9.4}_{-8.6}$	66 ± 12
UTfit	$21.42^{+0.91}_{-0.89}$	90.9 ± 8.0	70.8 ± 7.8

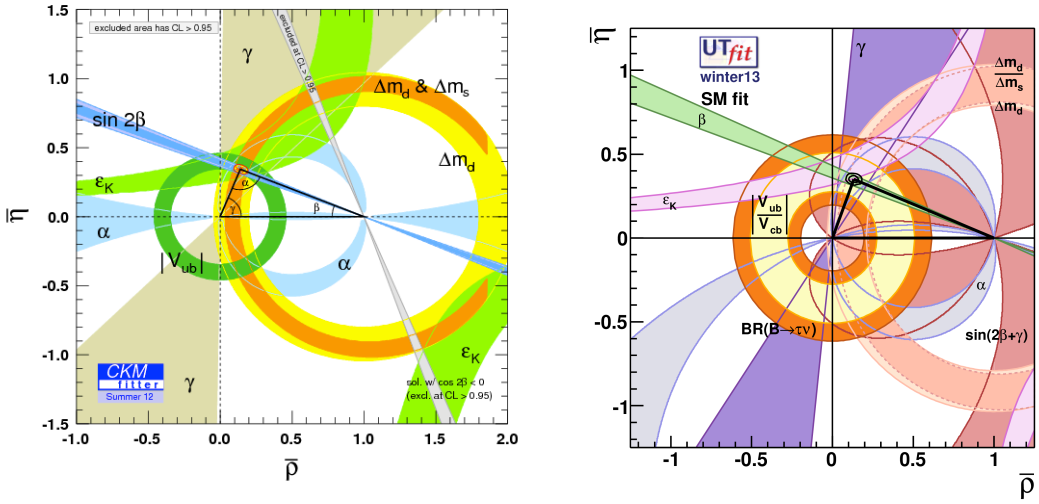

Figure 14. Global CKM fit results.

Table 7. Best fit values of the angles and apex of the Unitarity Triangle. Angle measurements are in degrees.

	CKMfitter	UTfit
β	$21.73^{+0.78}_{-0.74}$	21.95 ± 0.87
α	$90.5^{+4.3}_{-4.1}$	88.7 ± 3.1
γ	$67.7^{+4.1}_{-4.3}$	69.2 ± 3.2
$\bar{\rho}$	$0.140^{+0.027}_{-0.026}$	0.132 ± 0.021
$\bar{\eta}$	$0.343^{+0.015}_{-0.014}$	0.350 ± 0.014

specific fits to allow for generic New Physics effects have been performed to check the consistency of the full set of flavour measurements. Although there have been some hints of inconsistencies over the years, it appears that set of measurments made at the B factories and other flavour experiments are statistically consistent with Standard Model predictions.

8. Conclusions

Measurements of CP violation in B meson decays have been at the core of the B factories physics programs since their inception. A large number of independent measurements of CP-violating processes have been made, leading to precise determinations of the angles of the Unitarity Triangle. Together with non-CP-violating measurements, which tend to constrain the sides of the UT, these measurements have essentially verified the CKM mechanism of CP violation in the Standard Model. CP violation in B decays will continue to play an important role in flavour physics in the coming years. Many important measurements in the flavour sector are already being made at LHCb, while we can expect a significant improvement in the precision of many other measurements when the Belle 2 experiment turns on in a few years.

References

[1] J.H. Christenson, et al., Phys. Rev. Lett. **13**, 138 (1964).
[2] N. Cabibbo, Phys. Rev. Lett. **10**, 531 (1963).
[3] M. Kobayashi and T. Maskawa, Prog. Theor. Phys. **49**, 652 (1973).
[4] L. Wolfenstein, Phys. Rev. Lett. **51**, 1945 (1983).
[5] B. Aubert, et al. (Babar Collaboration), Nucl. Instr. Methods A **479**, 1 (2002).
[6] A. Abashian, et al. (Belle Collaboration), Nucl. Instr. Methods A **479** 117 (2002).
[7] I. Adachi, et al. (Belle Collaboration), Phys. Rev. Lett. **108**, 171802 (2012).
[8] B. Aubert, et al. (Babar Collaboration), Phys. Rev. D **79**, 072009 (2009).
[9] http://www.slac.stanford.edu/xorg/hfag/triangle/ichep2004/index.shtml#sin2b
[10] J.P. Lees, et al. (Babar Collaboration), Phys. Rev. D **85**, 112010 (2012).
[11] D. Atwood, et al., Phys. Rev. Lett. **78**, 3275 (1997),
A. Giri, et al., Phys. Rev. D **68**, 054018 (2003).
[12] P. del Ama Sanchez, et al. (Babar Collaboration), Phys. Rev. Lett. **105**, 121801 (2010).
[13] H. Aihara, et al. (Belle Collaboration), Phys. Rev. D **85**, 112014 (2012).
[14] M. Gronau, D. London and D. Wyler, Phys. Lett. B **253**, 483 (1991).
[15] P. del Amo Sanchez, et al. (Babar Collaboration), Phys. Rev. D **82**, 072004 (2010).
[16] Talk presented by K. Trabelsi at the CKM2012 Workshop, http://www.physics.uc.edu/~schwartz/CKM2012/program/
[17] http://www.slac.stanford.edu/xorg/hfag/triangle/summer2012/index.shtml#gamma_comb
[18] LHCb-CONF-2012-032, http://cds.cern.ch/record/1481337?ln=en
[19] I. Adachi, et al. (Belle Collaboration), BELLE-CONF-1211, arXiv:1302.0551.
[20] http://ckmfitter.in2p3.fr/www/studies/plots_ckm12/ckm_plots_ckm12.html
[21] http://ckmfitter.in2p3.fr/www/html/ckm_main.html
[22] http://utfit.org/UTfit/